Langmuir

ARTICLE

pubs.acs.org/Langmuir

Adsorption of *n*-Butanol from Dilute Aqueous Solution with Grafted Calixarenes

Anthony B. Thompson, Sydney J. Cope, T. Dallas Swift, and Justin M. Notestein*

Department of Chemical and Biological Engineering, Northwestern University, Technological Institute E136, 2145 Sheridan Road, Evanston, Illinois 60208, United States

ABSTRACT: Materials were synthesized for the recovery of *n*-butanol from dilute aqueous solutions, as may be useful for applications in biofuel−water separations. These materials are composed of hydrophobic, cavity-containing calixarenes covalently bound directly to porous, hydrophilic silica supports through a Si linker atom rather than a flexible organic linker, as is common, at surface coverages of up to ∼0.25 calixarenes/nm^2 (∼250 μmol calix/g matl). The calixarene ring size, upper rim groups, bridging group (calixarene vs thiacalixarene), and surface density were varied. The materials were characterized by NMR, UV−vis, and TGA. The absolute butanol uptake reached ∼0.16 mmol butanol per gram of material at equilibrium concentrations below 0.12 M and increased monotonically with the calixarene surface density. The background adsorption onto the silica surface was small at high calixarene loading. At 298 K, the free energy of adsorption in the calixarene cavities became more favorable by 3 kJ/mol as the surface area of the hydrophobic calixarene upper rim groups increased from H to methyl to *tert*-butyl, consistent with adsorption driven by van der Waals interactions. A thiacalix[4]arene-SiO_2 material, containing polarizable sulfur bridges and a larger, more conformationally mobile calixarene structure, had slightly stronger adsorption still. All materials except this thiacalixarene exhibited fully reversible adsorption into solution. As a representative material, the adsorption of *n*-butanol from aqueous solution at a *tert*-butylcalix[4]arene site was accompanied by a negligible enthalpy change but a small, favorable entropy change of +50 ± 20 J/mol/K, indicating that adsorption is driven by desolvation. Butanol desorbed from *tert*-butylcalix[4]arene materials at ∼150 °C into the gas phase, well within the range of stability of calixarenes (<300 °C), indicating that these materials have promise as regenerable adsorbents.

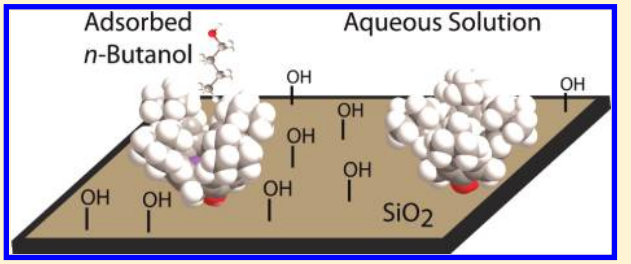

INTRODUCTION

Fermentation-derived butanol is a potential renewable fuel that has several advantages over other biofuels, including a higher energy density than ethanol and better solubility with current hydrocarbon fuels because of its relative nonpolarity. However, the recovery of the product from ABE fermentation broths is complicated by the low concentrations inherently yielded by the fermentation process because of the cytotoxicity of *Clostridium acetobutylicum* strains.[1] Because the normal boiling point of butanol is higher than that of water, the traditional recovery method of distillation requires high energy inputs from water boilup and is further complicated by a heterogeneous azeotrope at 365 K.[2] Overall, the energy demand is of comparable magnitude to the energy content of the product itself.[3] Common alternatives to distillation include pervaporation, liquid−liquid extraction, osmosis, and adsorption-based techniques.[1]

Butanol recovery by adsorption is predicted to have an average energy demand that is ∼10% of the heat of combustion of butanol and is easily implemented.[1] Common adsorbents typically investigated are activated carbons,[3] zeolites,[4] and polymers.[5] These adsorbents are generally inexpensive and have good capacity but are limited in their ability to be modified systematically on the molecular length scale. The alternative approach pursued here is to synthesize solid materials modified with organic groups that act as adsorption sites. Cavitands (intrinsically microporous organic molecules such as calixarenes and cyclodextrins) immobilized on solid supports make up one subclass of such materials that has been used in sensing, chromatography, and the separation of contaminants from wastewater[6−12] but remains relatively unexplored in the context of biofuel separations. Advantages to this approach of materials design are that (i) the structure and number of adsorption sites are, in principle, known *a priori* and tunable, (ii) understanding the adsorption behavior of the hybrid material is aided by solution and solid-state cavitand/guest complexation, and (iii) sites can be optimized for adsorption strength or selectivity independent of the optimization of the support for robustness and surface area.

Herein is presented the synthesis, characterization, and analysis of a class of adsorbents consisting of hydroxycalixarenes immobilized directly onto chlorinated silica surfaces.[7] Although calixarene-based adsorbents or separation media are known, the materials described here are distinguished by the lack of a flexible organic tether or polymer chain typically employed to attach the calixarene to the surface.[13] These directly attached calixarenes

Received: July 2, 2011
Revised: August 22, 2011
Published: August 23, 2011

Scheme 1. Grafting of a Calix[4]arene to a Silica Surface and an Illustration of the Grafted Conformation[a]

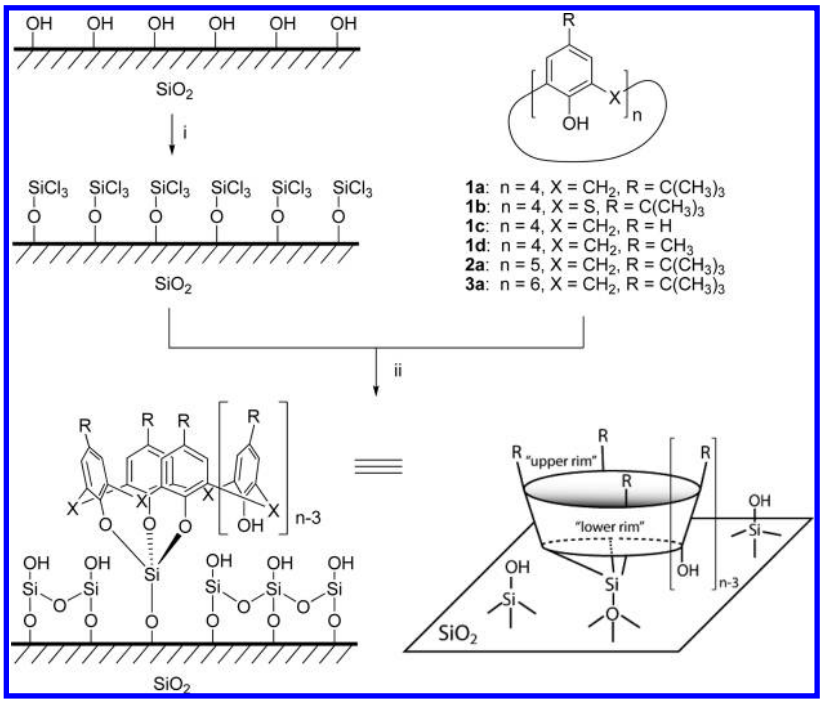

[a] (i) Shaken for 24 h at room temperature with 1:1 $SiCl_4/Et_3N$ in CH_2Cl_2. (ii) Refluxed for 24 h in toluene with 1.1:1 Et_3N/calixarene. The points of attachment in step ii are suggested to be three for calix[*n*]arenes and two for thiacalixarene **1b**, with reference to soluble complexes. See the text for a discussion. Some atoms are omitted for clarity on the bottom left.

have simplified syntheses and different surface chemistry. In addition to their use as tailorable adsorbents for biofuel separations, these materials also enable studies of the complexation behavior of hydrophobic calixarenes with guests in water, where the free calixarenes are generally poorly soluble without additional modification.[14] For example, the association between calixarenes and neutral alcohols in aqueous solution has been studied computationally,[15] but experimental measurements have not been possible to date.

EXPERIMENTAL METHODS

Synthesis. The calixarenes used in the materials syntheses are presented in Scheme 1. **1a** (MW = 649 g/mol) was purchased from Sigma-Aldrich, **1b** (MW = 721 g/mol) was purchased from TCI International, **2a** (MW = 811 g/mol) was purchased from Acros Organics, and **3a** (MW = 973 g/mol) was purchased from Alfa Aesar; all were used as received without further purification. **1c** (MW = 425 g/mol) was synthesized by the de-*tert*-butylation of **1a** following a previously published procedure.[16] **1d** (MW = 481 g/mol) was synthesized in a two-step process by the chloromethylation and subsequent dechlorination of **1c**, both following published procedures.[17] ^{1}H NMR spectra of synthesized **1c** and **1d** were consistent with the literature spectra. Porous silica gel, with a primary particle size of 100−200 μm and a BET surface area of 500 m^2/g, was obtained from Selecto Scientific and stored in an oven at 120 °C.

Triethylamine and toluene were freshly distilled from CaH_2 under N_2 before use. The silica starting material (typically 1.5 g, scalable up to 15.0 g without change) was dried under a dynamic vacuum of <50 mtorr at 250 °C for 24 h and then cooled to ambient temperature under N_2. Using standard air-free techniques, a 1 M solution of $SiCl_4$ in CH_2Cl_2 (6.8 mmol of $SiCl_4$ or 6.8 mL of solution per 1.5 g of SiO_2) was added, followed by the dropwise addition of triethylamine (6.8 mmol or 0.95 mL per 1.5 g of SiO_2). The flask was sealed under N_2 and shaken at 200 rpm for 24 h at room temperature, and then the solvent was evaporated and the material was dried under a dynamic vacuum of <50 mtorr at 70 °C for 24 h to yield a chlorinated silica gel, shown as the intermediate in Scheme 1. In a separate reaction vessel, excess calixarene (0 to 0.3 mmol per g of SiO_2) was dissolved in toluene (15 mL per g of SiO_2) at 120 °C. The chlorinated silica material was cooled to ambient temperature under N_2 and then poured into the calixarene solution, triethylamine was added (1.1 mol per mol of calixarene), and the mixture was refluxed under N_2 for >24 h on a shaker at 200 rpm. The purpose of shaking instead of stirring during synthesis was to reduce the grinding of silica particles by the stir bar, which decreased the amount of problematic fine powder and increased the synthesis yields.

Materials were then filtered and washed sequentially with (per 1.5 g of starting material) 100 mL of boiling toluene, 50 mL of methanol, 50 mL of 18.2 MΩ cm deionized water, 50 mL of methanol, 100 mL of acetonitrile, and 30 mL of petroleum ether. The materials were briefly dried in ambient air, Soxhlet extracted for 24 h with anhydrous benzene at 80 °C, and then dried under a dynamic vacuum of <50 mtorr at ambient temperature for 24 h. Next, the dry adsorbent materials were resuspended in 18.2 MΩ cm water, sonicated for 15 min, and then rinsed over a 230 standard mesh sieve with water to remove fine particles. Finally, the materials were dried under a dynamic vacuum of <50 mtorr at room temperature for 24 h and then dry sieved through a 120 standard mesh screen to remove large debris. The resulting beige to brown materials were stored in a desiccator at ambient temperature.

Characterization. Thermogravimetric analysis (TGA) was performed on a TA Instruments TGA Q500 operated in high-resolution mode with a temperature ramp of 10 °C/min to 800 °C under a flow of dry synthetic air in an alumina pan. Diffuse reflectance UV−vis spectra were obtained with a Shimadzu UV-3600 UV−vis spectrophotometer equipped with a Harrick praying mantis diffuse-reflectance accessory.

Table 1. List of All Materials with Respective Calixarene Contents

material	loading, σ (mmol/g)[b]	area density (nm^{-2})[c]	calixarene content (wt %)[d]
(000)[a]	0.00	0.00	0.0
1a(080)	0.08	0.10	4.9
1a(120)	0.12	0.14	7.2
1a(160)	0.16	0.19	9.4
1a(170)	0.17	0.20	9.9
1a(200)	0.20	0.24	11.5
1b(090)	0.09	0.11	6.1
1b(120)	0.12	0.14	8.0
1c(220)	0.22	0.26	8.5
1d(220)	0.22	0.26	9.6
2a(140)	0.14	0.17	10.2
3a(140)	0.14	0.17	12.0

[a] Baseline material, exposed to synthesis conditions but no added calixarene. [b] mmol calixarene/g of SiO_2. [c] Based on the original BET surface area of 500 m^2/g. [d] g of calixarene/100 g of total material.

Poly(tetrafluoroethylene) powder (Sigma-Aldrich) was used as a perfect reflector for calculating Kubelka−Munk pseudoabsorbance spectra. Solid-state carbon-13 cross-polarization/magic-angle spinning nuclear magnetic resonance (^{13}C CP/MAS NMR) spectra were obtained on a 400 MHz Varian spectrometer at a spin rate of 5 kHz. Solution-phase proton nuclear magnetic resonance (^{1}H NMR) spectra (for characterizing synthesized calixarenes **1c** and **1d** and the precursor to **1d**) were obtained in $CDCl_3$ on a Varian Inova 500 MHz spectrometer.

Butanol Adsorption. All adsorption experiments were initiated by placing known masses of material (50 to 100 mg) in a series of 1 dram glass vials with fluoropolymer-lined screw caps, adding the aqueous butanol solutions (1 to 2 mL, 0 to 0.12 M) with an autopipettor, and sonicating for 30 min. The samples were then equilibrated for 24 h on a shaker at 200 rpm. Heating was achieved with a resistance-heated aluminum block, and cooling was achieved with an aluminum block connected to a chiller (VWR model 1140S, temperature controlled to ±0.5 °C). The solutions were separated from the suspension using glass microfiber syringe filters (Whatman binder-free grade GF/F 13 mm, polypropylene housing, pore size 0.7 μm). For non-ambient-temperature experiments, equilibrium solutions were separated and then resealed in vials and allowed to cool or warm to room temperature before analysis. Saturated concentrations of butanol in water were calculated by fitting a third-order polynomial to tabulated values.[18]

Equilibrium butanol concentrations were determined via the refractive index at 20 °C measured with an Atago RX-007α temperature-controlled benchtop refractometer, which was calibrated against a series of known-concentration stock solutions in the range of 0.00 to 0.20 M, accurate to ±0.00065 M. Calculations of the equilibrium concentration were corrected by the change in refractive index of a control sample containing only water and calixarene material that was equilibrated alongside the butanol-containing samples. After the extensive washing discussed in the Synthesis subsection, this background correction was small compared to refractive index changes caused by the decrease in the liquid-phase butanol concentration.

Solution Desorption. For each material, two sample vials were prepared: one containing a known amount of water and adsorbent (0.5−1.0 mL and 50−100 mg, respectively) and another containing the same volume of 0.125 M butanol solution and nearly the same mass of material. The two samples were sonicated for 30 min and then equilibrated on a shaker for 24 h at room temperature. After the samples were allowed to settle for 10 min, a known amount of liquid (corresponding to most of the liquid present) was extracted from each vial with a syringe, filtered with a glass fiber syringe filter, and then analyzed. A known amount of pure water (1 to 2 mL) was then added to each vial; the vials were shaken for 24 h and analyzed as before. The refractive index of the butanol-containing sample was then corrected by the change in the refractive index of the sample containing only water; these corrections were small as a result of extensive washing of the synthesized materials.

Temperature-Programmed Desorption. Temperature-programmed desorption (TPD) experiments were carried out in 90 cm^3/min N_2 on a TA Instruments TGA Q500 connected to a Pfeiffer ThermoStar GSD301-T2 mass spectrometer. The TGA was programmed with a linear temperature ramp of 5 °C/min to 300 °C in an alumina pan while mass fragments corresponding to butanol (m/z = 31, 41, 56) and water (m/z = 17 and 18) were monitored continuously. The sample consisted of **1a(160)** that had been equilibrated for 24 h in a saturated solution of butanol in water. The material was filtered and placed in the TGA pan after brief air drying. An initial 100 min isothermal step at room temperature removed weakly physisorbed species. A control sample consisting of the material equilibrated in water and another control sample of dry material only were run under the same conditions and showed no signals at m/z = 31, 41, or 56.

RESULTS AND DISCUSSION

Characterization. This synthesis methodology immobilizes calixarenes[6] and other cavitands[19] by covalent O−Si bonds at the lower rim (Scheme 1). The proposed number of these covalent connections is made by analogy to well-characterized small-molecule complexes. Calix[4]arenes typically react with silyl chlorides to generate tripodal structures,[20−23] whereas the only reported analogous reactions with thiacalix[4]arene involve only two adjacent phenols.[24] Likewise, it is suggested that grafted calix[n]arenes **1a**, **1c**, **1d**, **2a**, and **3a** are attached at three points whereas thiacalix[4]arene **1b** is attached at two. As a corollary, this imparts a relatively greater conformational flexibility to the latter surface species. In contrast to immobilization schemes using a long organic tether, this method should immobilize the hydrophobic cavities facing outward from the surface, and the single Si atom anchoring the calixarene to the surface also prevents the calixarene from undergoing larger conformation changes that would eliminate the central cavity (e.g., to a 1,3-alternate form) in water. The highest surface densities achieved here correspond to ∼40% of a complete monolayer, which is near the maximum that one would expect from random, irreversible grafting. It must be noted that the surface attachment afforded by the multiple phenols of the calixarene macrocycle resulted in a much more stable surface layer than the corresponding monodentate phenols. For example, these deliberately harsh washing and sonication pretreatments completely removed any monomeric *tert*-butylphenol that was grafted by analogous procedures.

A characteristic TGA weight loss curve and its temperature derivative (absolute value) are shown in Figure 1. The mass loss centered at 100 °C is attributed to physisorbed water, and the loss from 300 to 800 °C corresponds to the combustion of calixarenes and small amounts of adsorbed species from synthesis. To calculate calixarene loadings, weight loss curves were normalized by the weight at 300 °C and then the baseline **(000)** curve was subtracted. The remaining weight loss was assumed to be combustion of the calixarene and was converted to a surface loading using the molecular weight of the particular calixarene.

Characteristic diffuse reflectance UV−vis spectra are shown in Figure 2 for **1a(160)**, **(000)**, and pure powdered calixarene **1a**.

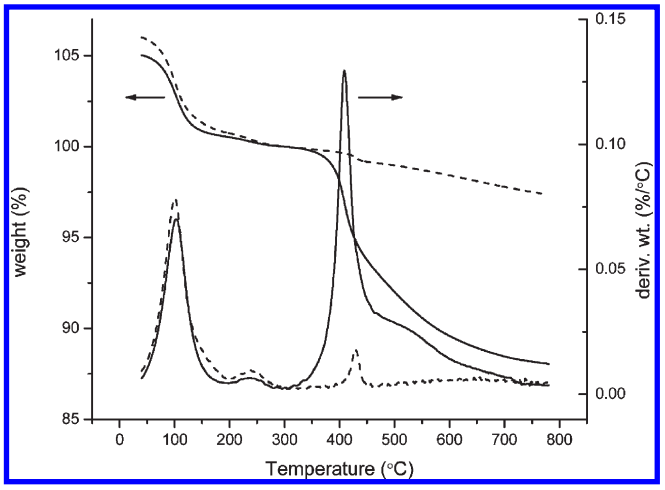

Figure 1. TGA weight loss curves and temperature derivatives, **1a(160)** (—) and **(000)** (---). Arrows indicate the respective axes.

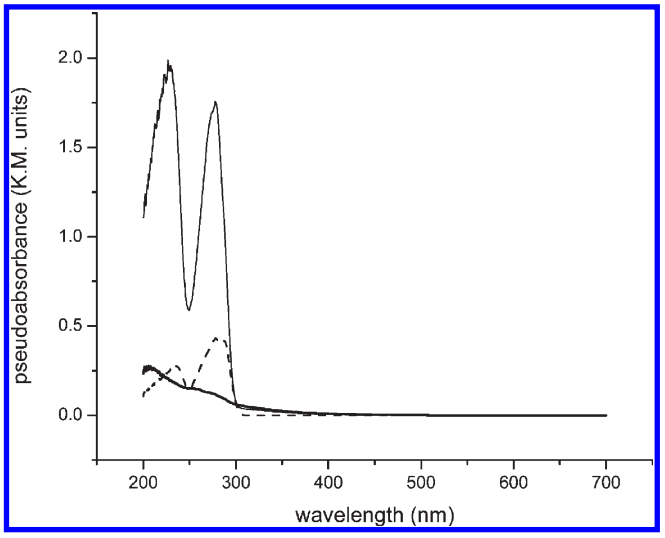

Figure 2. Diffuse-reflectance UV—vis pseudoabsorbance spectra for pure powdered calixarene **1a** (---, diluted to 5 wt % in PTFE), baseline material **(000)** (—, diluted to ~30 wt % in PTFE), and material **1a(160)** (—, diluted to 5 wt % calixarene or ~30 wt % silica in PTFE).

The peak near 280 nm is characteristic of the aromatic core of the calixarene. Figure 3 shows solid-state ^{13}C CP/MAS NMR of **1a(200)**. The larger peak near 30 ppm corresponds to methyl carbons in the *tert*-butyl group, and the smaller peak corresponds to the bridging methylene carbons. The *tert*-butyl quaternary carbon is obscured by the larger peaks. Peaks at 130 and 150 ppm correspond to the phenyl carbons.

Adsorption Modeling. Adsorption from binary liquid mixtures onto solids is often described using surface-excess-type isotherms,[25] which are useful in describing energetically heterogeneous surfaces such as activated carbons[26] but typically lack the concept of an adsorption site, as in the BET or Langmuir-type models for gas-phase adsorption.[27] For a single solute near the infinite dilution limit, however, the isotherm equations are identical to those used for the adsorption of single gases,[28] with the adsorbate activity equal to the reduced pressure relative to the saturation vapor pressure or reduced concentration relative to

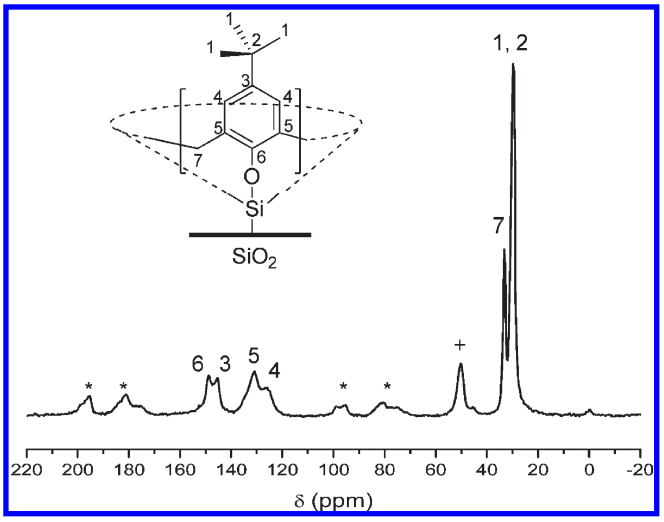

Figure 3. Solid-state ^{13}C CP/MAS NMR spectrum of **1a(200)** collected at a spin rate of 5 kHz. Spinning sidebands are denoted by asterisks (*), and surface methoxy species derived from methanol washing are denoted by pluses (+).

the concentration at saturation. These isotherms have been used to describe adsorption from dilute aqueous solutions in many cases;[29−32] for example, Jaroniec, Dabrowski, and Toth[30] modeled the adsorption of *n*-amyl alcohol and other organic solutes onto carbon with BET-type equations, and Radke and Prausnitz[31] used a Langmuir—Freundlich model to describe the adsorption of isopropanol and other solutes from water onto activated carbon.

In this study, a grafted calixarene is defined to be a single adsorption site having a characteristic energy of adsorption. Although the assumptions of a BET-type model are often unrealistic, they are appropriate here because (i) there is a known number of independent adsorption sites as defined by the number of grafted calixarenes, (ii) adsorbates at one calixarene site are not expected to interact laterally with other adsorbates because the calixarene adsorption sites are themselves separated from one another, and (iii) multilayer formation is expected to "stack" at hydrophobic calixarene sites rather than spread evenly to the hydrophilic support. Thus, the adsorption of butanol to calixarene—silica materials is modeled by an equation for multilayer isotherms derived in the original study by Brunauer, Emmett, and Teller,[27] which allows for differences in the adsorbate capacity and heat of adsorption between the first and second to subsequent layers. The fractional uptake θ is given by

$$\theta = \frac{q}{\sigma} = \frac{cx}{1-x}\left(\frac{1 + (\varepsilon b - 1)(2-x)x}{1 + (c-1)x + (b-1)cx^2}\right) \qquad (1)$$

where

$$c \equiv \exp\left(-\frac{\Delta G_1 - \Delta G_L}{RT}\right),$$

$$b \equiv \exp\left(-\frac{\Delta G_2 - \Delta G_L}{RT}\right), \text{and } x \equiv \frac{C_{eq}}{C_o(T)} \qquad (2i - 2iii)$$

Here, q (mmol of BuOH/g of matl) is the observed total uptake, σ (mmol of calixarene/g of matl) is the calixarene surface loading defined by synthesis, ΔG_1 and ΔG_2 (kJ/mol) are the net free energies of adsorption in the first and second layers, ΔG_L

dx.doi.org/10.1021/la202508q |*Langmuir* 2011, 27, 11990–11998

(kJ/mol) is the free energy of transfer into a saturated surface layer, which in this context is comparable to the opposite of the free energy of solvation at infinite dilution (at 298 K, ΔG_L = −9.76 kJ/mol, ΔH_L = +9.28 kJ/mol, and ΔS_L = +64 J/mol/K[33]), C_{eq} (M) is the observed equilibrium butanol concentration, $C_0(T)$ (M) is the saturated concentration of *n*-butanol in water at temperature T (K), and ε is the ratio of second-layer sites to those in the first (i.e., the inverse of parameter δ in the original BET study[27]). In the original derivation, $x = p/p_0$, the ratio of pressure to the saturated vapor pressure of the adsorbate; however, for systems that obey the linear dependence between the partial pressure and the liquid-phase mole fraction of the sorbate, such as the *n*-butanol−water system at the low concentrations considered,[34] eq 2iii is equivalent to $x = p/p_0$.

Here, we consider the first layer to consist of the known number of calixarene cavities (per gram) σ; adsorption into these cavities is described by c. We consider the second layer to be the unknown number of adsorption sites exterior to the calixarene cavities, which includes adsorption on residual silica and weaker secondary adsorption on the calixarenes (but presumably exo to the cavity); this adsorption is described by b. To reduce the number of fitting parameters, ε is allowed to vary, but adsorption on the sites exterior to the calixarene cavities is assumed to be weak and comparable to the nonspecific formation of the saturated surface layer (or $c \gg b \approx 1$). Considering also that x is small (<0.12) in all cases considered, eq 1 reduces to eq 3, which is used to describe the adsorption data herein. Note that the mole fraction of butanol is <0.002 for all experiments in this report, and this system is operating near the infinite dilution limit.

$$\theta = \frac{q}{\sigma} = \frac{cx}{1-x}\left(\frac{1 + (\varepsilon - 1)(2-x)x}{1 + (c-1)x}\right) \qquad (3)$$

For consistency, the baseline silica material (**000**) is described by a standard BET isotherm,

$$q = \frac{q_m a x}{(1-x)(1 + (a-1)x)} \text{ where}$$

$$a \equiv \exp\left(-\frac{\Delta G_{SiO_2} - \Delta G_L}{RT}\right) \qquad (4i \text{ and } 4ii)$$

with ΔG_{SiO_2} denoting the free energy of adsorption on the material surface and q_m representing the monolayer capacity. Because the baseline material contains no exocalixarene sites, as mentioned above, parameter a is not exactly equivalent to b in eqs 1 and 2i−2iii. The goal of this modeling effort is primarily to provide a method of internal comparisons for adsorption specifically at the calixarene sites. Further modeling for the prediction of total uptake under different processing conditions is reserved for the future.

Effect of the Calixarene Surface Density. Ambient-temperature adsorption experiments were conducted with **1a** at different surface densities on SiO_2 in order to determine the effect of calixarene loading on uptake. Data was fitted by a nonlinear least-squares regression to eq 3: first, the curves were fit while allowing the ε and c parameters to vary, and then an average value of c was calculated and the curves were refit with the fixed c. The c parameter should be intrinsic to the calixarene and thus should not vary with the calixarene surface density. The data, expressed as the absolute uptake (Figure 4A), indicate that butanol uptake increases with the surface density, as would be expected for hydrophobic cavities containing *tert*-butyl groups capable of hydrophobic interactions with *n*-butyl chains.

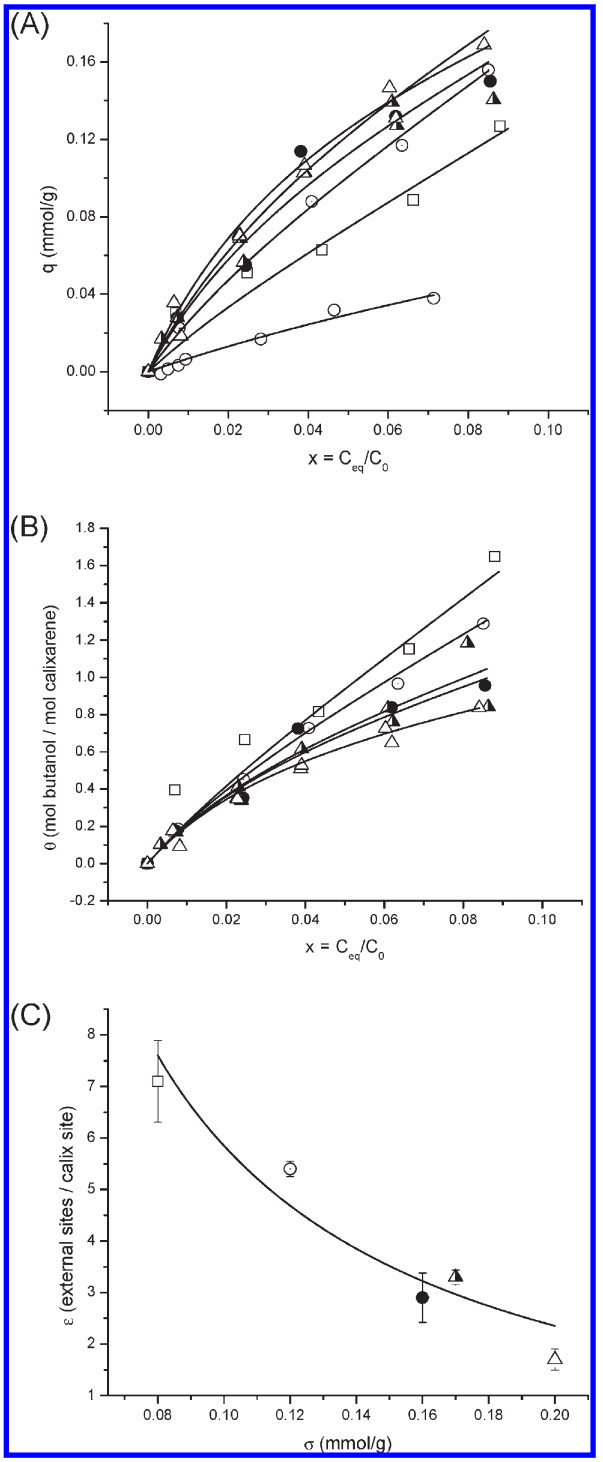

Figure 4. Equilibrium room-temperature adsorption isotherms [○ = (**000**), □ = **1a**(**080**), ⊙ = **1a**(**120**), ● = **1a**(**160**), ▲ = **1a**(**170**), and △ = **1a**(**200**)], expressed as (A) the absolute uptake and (B) the fractional uptake. Fit parameters to eq 3 are given in Table 2. (C) Ratio of noncavity adsorption sites to calixarene cavity sites, ε, as a function of loading σ. The line is a guide to the eye.

Conversely, when normalized by the calixarene loading (Figure 4B), the data set collapses to a set of lines with the same initial slope (equal to the c constant) that diverges at higher

dx.doi.org/10.1021/la202508q |*Langmuir* 2011, 27, 11990–11998

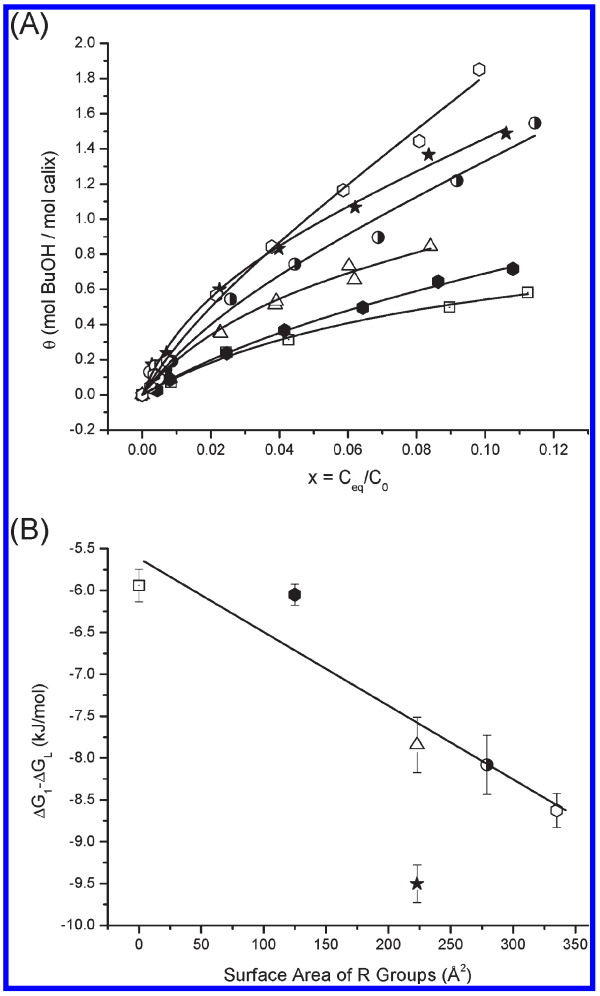

Figure 5. (A) Equilibrium room-temperature adsorption isotherms [Δ = **1a(200)**, ★ = **1b(120)**, ⊡ = **1c(220)**, ⬢ = **1d(220)**, ◑ = **2a(140)**, and ⬡ = **3a(140)**] normalized by the calixarene surface density. The fit parameters to eq 3 are given in Table 2. (B) Free energies of adsorption as calculated from parameter *c* and given as a function of the combined molecular surface area of calixarene R groups. The fitted line shows that thiacalix[4]arene **1b(120)** is an obvious outlier.

concentrations. The higher-surface-density materials appear to plateau at increasing concentration, indicating that most of the butanol uptake is occurring at the calixarene sites, which are beginning to saturate. This effect is observed in a plot of the site ratio ε versus the calixarene loading σ (Figure 4C) where ε, the relative number of weaker adsorption sites external to the calixarene cavity, decreases with increasing surface density σ. Because the first layer capacity is defined as the calixarene loading, the second layer inherently represents all external adsorption sites, including those on the residual oxide surface as well as any noncavity sites associated with calixarenes (for example, on the outer surface of the *tert*-butyl groups of **1a**). The latter also includes interstitial sites between adjacent grafted calixarenes. Figure 4C shows that ε drops below 2 at high calixarene loading. Additional surface modifications are being explored to decrease this value further.

Effect of Calixarene Structure. At the maximum calixarene surface density, the role of the residual silica surface is minimized, allowing the effects of the calixarene chemical structure to be seen most easily. The lack of a flexible organic tether connecting the calixarene to the silica is also important because it eliminates

Table 2. Fit Parameters for Room-Temperature Adsorption (298 K)[a]

material	*c* (nd)	ε (nd)	$\Delta G_1 - \Delta G_L$ (kJ/mol)
1a(080)	24 ± 3	7.1 ± 0.8	−7.8 ± 0.4
1a(120)	24 ± 3	5.4 ± 0.2	−7.8 ± 0.4
1a(160)	24 ± 3	2.9 ± 0.5	−7.8 ± 0.4
1a(170)	24 ± 3	3.3 ± 0.1	−7.8 ± 0.4
1a(200)	24 ± 3	1.7 ± 0.2	−7.8 ± 0.4
1b(090)	46 ± 4	3.8 ± 0.2	−9.5 ± 0.3
1b(120)	46 ± 4	4.0 ± 0.2	−9.5 ± 0.3
1c(220)	11 ± 1	0.4 ± 0.2	−5.9 ± 0.2
1d(220)	12 ± 1	1.6 ± 0.2	−6.1 ± 0.1
2a(140)	26 ± 4	4.2 ± 0.5	−8.1 ± 0.4
3a(140)	33 ± 3	6.7 ± 0.3	−8.6 ± 0.2
	a (nd)	q_m (mmol/g)	$\Delta G_{SiO_2} - \Delta G_L$ (kJ/mol)
(000)	6 ± 4	0.12 ± 0.06	−4.4 ± 2.7

[a] *c* was calculated from the nonlinear regression to eq 3, and the free energies of adsorption were calculated from eqs 2i−2iii. The parameters for **(000)** were calculated from eqs 4i and 4ii.

a competing adsorption site. Figure 5A compares the σ-normalized room-temperature adsorption isotherms for materials near the maximum loading of each calixarene.

From Figure 5A, H-calix[4]arene-SiO_2 material **1c(220)** clearly has a lower affinity for butanol than do all other materials except the baseline **(000)**. This suggests that the upper-rim calixarene functional groups contribute substantially to the degree of uptake, but the phenolic walls of the calixarene cavity could also play an important role. A comparison of curves **1a(200)**, **1c(220)**, and **1d(220)**, in which the only difference in calixarene structure is the R group, shows that the uptake increases as the size of the hydrophobic R group changes from H to methyl to *tert*-butyl. Comparing curves **1a(200)**, **2a(140)**, and **3a(140)**, in which the only difference is the number of phenolic units in the calixarene macrocycle, it is evident that the uptake increases with the size of the cavity or the number of bulky *tert*-butyl groups at the upper rim. These results suggest that differences in adsorption between materials are driven in large part by nonspecific van der Waals interactions occurring between the *n*-butyl chain of butanol and the alkyl R groups on the calixarene upper rim. This is consistent with the linear correlation (Figure 5B) observed between the free energies of adsorption (from fitted *c* values in Table 2) and the relative molecular surface area of the R groups (Connolly accessible area, 1.4 Å probe radius), where thiacalixarene material **1b(120)** is a far outlier. The differences are discussed below.

The effect of bridging group X (Scheme 1) can be seen by comparing curves **1a(200)** and **1b(120)**, where the only difference in the calixarene structure is the bridging species. Clearly, material **1b(120)** with sulfur bridging atoms produces a much higher uptake than does material **1a(200)** with methylene bridging groups, despite having the same number of phenolic subunits and *tert*-butyl groups at the upper rim. This difference attests to the special role of the preorganization of the *tert*-butylphenol groups into a macrocycle, and the difference is possibly due to the more open structure of **1b** as compared to that of **1a**, which has been observed in crystal structures[35] and

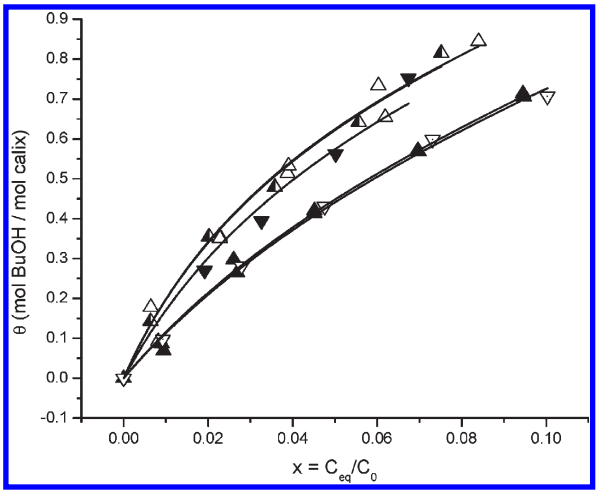

Figure 6. Equilibrium adsorption isotherms for **1a(200)** at 278 K (▼), 288 K (◭), 298 K (Δ), 308 K (▲), and 318 K (▽).

Table 3. Fit Parameters for Adsorption on 1a(200) at Different Temperatures[a]

T (K)	c (nd)	$\Delta G_1 - \Delta G_L$ (kJ/mol)
278	20 ± 2	−6.9 ± 0.2
288	24 ± 1	−7.6 ± 0.1
298	24 ± 3	−7.8 ± 0.4
308	12 ± 1	−6.5 ± 0.1
318	12 ± 1	−6.6 ± 0.1

[a] Curves were fit with the ε value (1.7) for **1a(200)** from Table 2.

results partially from the increased bond length from carbon to sulfur. It is observed here that the grafted structure of **1b** takes up much more surface area than does **1a** (lower maximum surface coverage achieved with **1b** vs **1a**). This extended structure would leave more space between *tert*-butyl groups at the upper rim, increasing the area available to make van der Waals contacts with butanol alkyl chains. It is also possible that the larger cavity is able to accommodate higher than 1:1 guest/calixarene ratios, which was observed in water-soluble complexes of thiacalix[4]arene−tetrasulfonate with various guests having a higher average guest/calixarene ratio than the corresponding methylene-bridged calixarene.[35] Finally, an open structure and the presence of polarizable S groups in the thiacalixarene could enable OH(butanol)−O(calixarene), OH(butanol)−S(calixarene) or CH(butanol)−π(calixarene) interactions between calixarene and butanol adsorbed deeply into the cavity. These types of interactions have been observed through proton NMR and CD spectroscopy between various aliphatic alcohols and resorcinarenes in chloroform solution.[36]

Temperature Effects. Figure 6 shows adsorption isotherms collected for **1a(200)** from 278 to 318 K, plotted against solubility-normalized concentrations $x = C_{eq}/C_0(T)$. The temperature dependence of parameter c allows for the determination of the average enthalpy and entropy of interaction between butanol and calixarene sites through the the van't Hoff equation,

$$\frac{d(\ln\ c)}{d(1/T)} = -\frac{\Delta H_1 - \Delta H_L}{R} \qquad (6)$$

which is combined with eqs 2i−2iii and written in linear form:

$$\ln c = -\frac{\Delta H_1 - \Delta H_L}{RT} + \frac{\Delta S_1 - \Delta S_L}{R} \qquad (7)$$

It must be recalled that plotting the uptake against the normalized concentration removes the temperature dependence of butanol desolvation from water. From Figure 6, changes in uptake versus temperature indicate that adsorption on **1a** is slightly exothermic (−11 ± 6 kJ/mol) and has negligible differences in entropy (−15 ± 20 J/mol/K) relative to the formation of a saturated surface layer. Using the values for ΔH_L and ΔS_L proposed above, the adsorption at the calixarene site is near thermoneutral and has a favorable entropy of adsorption of +50 ± 20 J/mol/K. These values suggest that adsorption on these materials is driven by desolvation and the hydrophobic effect rather than a strong molecular interaction.

Reversibility of Adsorption. The reversibility of adsorption was tested to verify that equilibrium isotherms were being measured and that the materials could be regenerated during real-world application. Figure 7A shows that butanol adsorption was reversible within error for materials derived from methylene-bridged calixarenes **1a** and **3a**. Dilution from a point of high uptake tracked the isotherms previously collected from individual uptake experiments. In contrast, thiacalixarene material **1b(090)** did not reversibly adsorb butanol, giving an uptake after dilution that is substantially higher than the previously obtained isotherm (Figure 7B). Uptake from the diluted solution was also greater than the calixarene loading, which could indicate that only the weakly adsorbed second layer was reversible. Irreversible adsorption at the calixarene may be attributed to the greater conformational flexibility of **1b** relative to **1a**, as shown by others using NMR,[37] and further enabled by the possibility of fewer connections to the surface for **1b** as compared to the number for **1a**. This conformational mobility may allow the calixarene to adjust its cavity size upon inclusion of a butanol molecule in order to increase the hydrophobic contact area and thus the strength of binding, resulting in the observed hysteresis. These materials are under further investigation.

Figure 8A shows the derivative weight change, and Figure 8B shows the mass spectrometer ion current signals for butanol (m/z = 41) and water (m/z = 18) during the temperature-programmed desorption of butanol and water from **1a(160)**. From the ion signals, it is clear that the second peak in the weight loss corresponds to a loss of butanol. The maximum rate of butanol weight loss occurs at ∼152 °C, which is approximately 34 °C above its normal boiling point. The area under that part of the curve corresponds to ∼0.05 mmol/g (∼0.30 mol butanol/mol calixarene). This experiment shows that a portion of the butanol is present on the surface as strongly adsorbed species and a greater portion is more weakly adsorbed and able to be removed during the initial isothermal step. This is consistent with our picture of the material consisting of a number of strongly adsorbing calixarene sites, surrounded by approximately three times as many (for this material) sites that do not interact with butanol any more strongly than the energy of desolvation.

Possible Host−Guest Complex Structures. Owing to the poor solubility of hydrophobic calixarenes in water, little is known about their complexation behavior with alcohols from aqueous solution. Crystal structures and solid-state NMR experiments with *n*-butanol and **1a** found that the cavity had no preference for OH over CH (but an affinity for both).[8] In aqueous solution, however, studies are limited to calixarenes solubilized with polar R

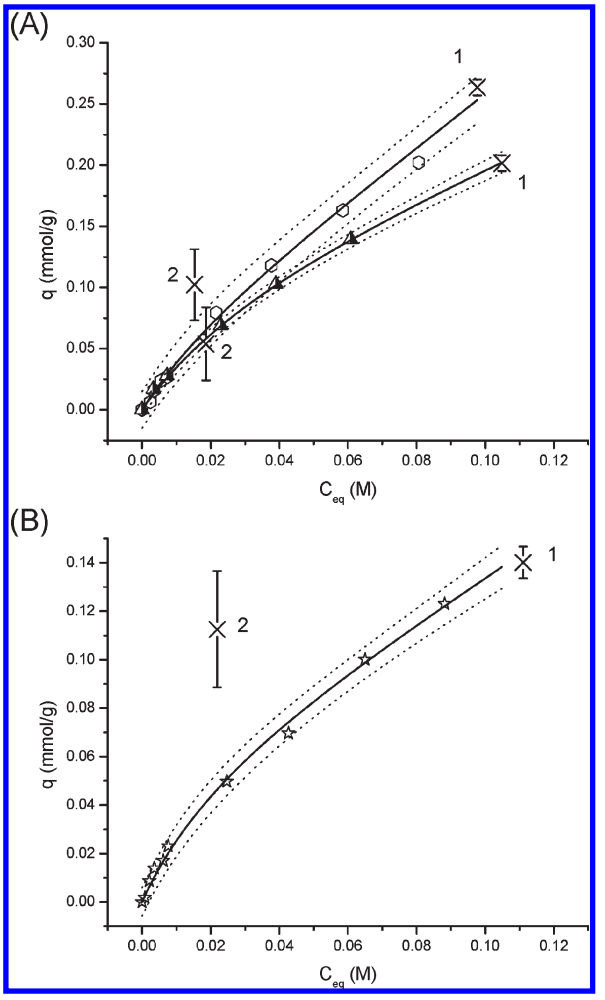

Figure 7. Desorption experiments (data denoted by ×) overlaid on previously obtained room-temperature equilibrium isotherms [(A) ▲ = **1a(170)**, ⬡ = **3a(140)**; (B) ☆ = **1b(090)**]. Point 1 is the first equilibration, point 2 is after the dilution of the solution and reequilibration. Dotted lines indicate 95% prediction bands. The error is ±5% from volume measurements.

groups such as SO_3^-. Alcohol−calixarene endocomplexes with the butanol OH moiety oriented outward were observed by NMR,[38] and complexes with homologous alcohols and diols were modeled with molecular dynamics;[15] in both instances, however, the complex was driven by charge assistance from the sulfonate groups at the upper rim, thus limiting the relevance of comparisons. Here it is suggested that butanol may adsorb with the alkyl tail included in the cavity. This would enable the CH(butanol)−π(calixarene) interaction mentioned previously, avoid unfavorable aqueous solvation of the alkyl tail, and allow the butanol hydroxyl to hydrogen bond with water. Simulations are underway to understand candidate structures.

CONCLUSIONS

Calixarenes have been directly grafted to an otherwise hydrophilic SiO_2 surface, fully characterized, and used in the adsorption of *n*-butanol from dilute aqueous solution. These studies demonstrate the potential application for the separation of biofuels from fermentation broths. Adsorption energies and uptakes generally become more favorable with the number of hydrophobic contacts present on the upper rim of the calixarene.

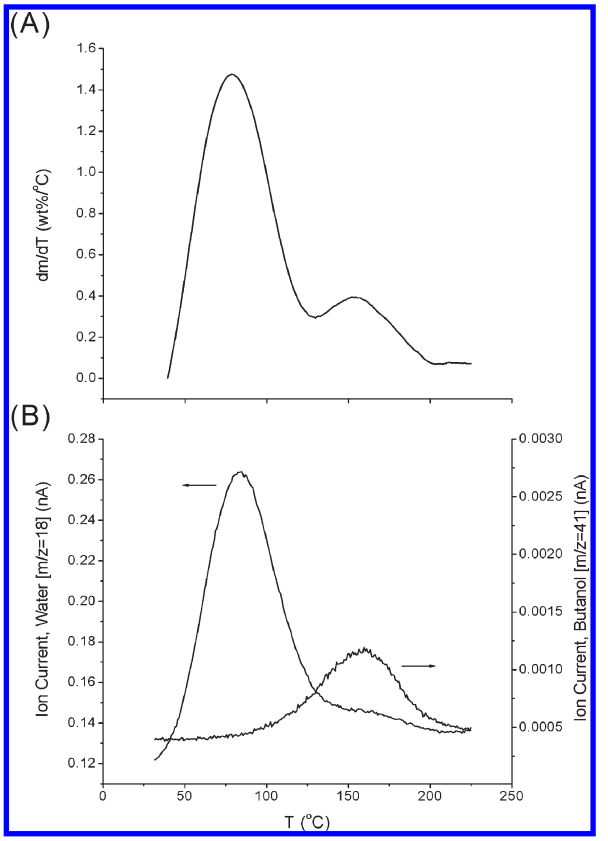

Figure 8. (A) Temperature derivative of the TGA weight loss curve for desorption experiment on **1a(160)**, with units in the weight percent of total desorbed mass, not the total mass of the sample. (B) Mass spectrometer signals for butanol and water fragments. Arrows indicate respective axes.

As such, adsorption is expected to be largely driven by nonspecific van der Waals interactions, but the possibility of significant contributions from CH−π or OH−π interactions cannot be dismissed. The adsorption on **1a** materials is fully reversible and is slightly more exothermic and less entropically favorable than phase separation from an infinitely dilute solution. These thermodynamics are also consistent with nonspecific interactions between butanol and the calixarene cavity. Exceptions to these statements are materials from thiacalixarene **1b**, which shows irreversible behavior and a stronger uptake than its analogue **1a**. The flexibility and the polarizable groups in this calixarene may be contributing to this behavior, which is being explored further. Calixarenes are stable up to ∼300 °C and butanol is desorbed from the cavity of **1a** at ∼150 °C, thus the materials are capable of regeneration. Finally, the synthesis protocols presented here can be generalized to a wide variety of functionalized calixarenes and supports, which may lead to new, selective adsorbents in the future and a better understanding of calixarene host−guest chemistry.

AUTHOR INFORMATION

Corresponding Author

*E-mail: j-notestein@northwestern.edu.

ACKNOWLEDGMENT

The National Science Foundation is acknowledged for grant CBET 0933667. Additional funding was provided by the

Initiative for Sustainability and Energy at Northwestern (ISEN) and the Northwestern University Materials Research Science and Engineering Center (MRSEC), funded under NSF award number DMR-0520513. NMR at the Integrated Molecular Structure Education and Research Center (IMSERC) at Northwestern University is supported by the NSF (DMR-0521267, solid-state NMR) and a donation from Pfizer, Inc. (solution NMR).

REFERENCES

(1) Oudshoorn, A.; van der Wielen, L. A. M.; Straathof, A. J. J. Assessment of options for selective 1-butanol recovery from aqueous solution. *Ind. Eng. Chem. Res.* **2009**, *48*, 7325–7336.

(2) Haynes, W. M., Ed. *CRC Handbook of Chemistry and Physics*, 91st ed.; CRC Press/Taylor & Francis: Boca Raton, FL, 2011.

(3) Qureshi, N.; Hughes, S.; Maddox, I. S.; Cotta, M. A. Energy-efficient recovery of butanol from model solutions and fermentation broth by adsorption. *Bioprocess Biosyst. Eng.* **2005**, *27*, 215–222.

(4) Oudshoorn, A.; van der Wielen, L. A. M.; Straathof, A. J. J. Adsorption equilibria of bio-based butanol solutions using zeolites. *Biochem. Eng. J.* **2009**, *48*, 99–103.

(5) Nielsen, D. R.; Prather, K. J. In situ product recovery of n-butanol using polymeric resins. *Biotechnol. Bioeng.* **2009**, *102*, 811–821.

(6) Notestein, J. M.; Katz, A.; Iglesia, E. Energetics of small molecule and water complexation in hydrophobic calixarene cavities. *Langmuir* **2006**, *22*, 4004–4014.

(7) Katz, A.; Da Costa, P.; Lam, A. C. P.; Notestein, J. M. The first single-step immobilization of a calix-[4]-arene onto the surface of silica. *Chem. Mater.* **2002**, *14*, 3364–3368.

(8) B. Brouwer, E.; A. Udachin, K.; D. Enright, G.; I. Ratcliffe, C.; A. Ripmeester, J. A chlorophobic pocket in the p-tert-butylcalix[4]arene cavity: a test site for molecular recognition investigated by ^{13}C CP MAS NMR and X-ray crystallography. *Chem. Commun.* **1998**, *5*, 587–588.

(9) Chen, M.; Chen, Y.; Diao, G. Adsorption kinetics and thermodynamics of methylene blue onto *p-tert*-butyl-calix[4,6,8]arene-bonded silica gel. *J. Chem. Eng. Data* **2010**, *55*, 5109–5116.

(10) Brindle, R.; Albert, K.; Harris, S. J.; Troltzsch, C.; Horne, E.; Glennon, J. D. Silica-bonded calixarenes in chromatography I. Synthesis and characterization by solid-state NMR spectroscopy. *J. Chromatogr., A* **1996**, *731*, 41–46.

(11) Gorbatchuk, V. V.; Tsifarkin, A. G.; Antipin, I. S.; Solomonov, B. N.; Konovalov, A. I.; Seidel, J.; Baitalov, F. Thermodynamic comparison of molecular recognition of vaporous guests by solid calixarene and diol hosts. *J. Chem. Soc., Perkin Trans. 2* **2000**, 2287–2294.

(12) Schierbaum, K. D.; Weiss, T.; Vanvelzen, E. U. T.; Engbersen, J. F. J.; Reinhoudt, D. N.; Gopel, W. Molecular recognition by self-assembled monolayers of cavitand receptors. *Science* **1994**, *265*, 1413–1415.

(13) Sokoließ, T.; Schönherr, J.; Menyes, U.; Roth, U.; Jira, T. Characterization of calixarene- and resorcinarene-bonded stationary phases: I. Hydrophobic interactions. *J. Chromatogr., A* **2003**, *1021*, 71–82.

(14) Böhmer, V. Calixarenes, macrocycles with (almost) unlimited possibilities. *Angew. Chem., Int. Ed. Engl.* **1995**, *34*, 713–745.

(15) Ghoufi, A.; Morel, J. P.; Morel-Desrosiers, N.; Malfreyt, P. MD simulations of the binding of alcohols and diols by a calixarene in water: connections between microscopic and macroscopic properties. *J. Phys. Chem. B* **2005**, *109*, 23579–23587.

(16) Gutsche, C. D.; Lin, L. G. Calixarenes 12: the synthesis of functionalized calixarenes. *Tetrahedron* **1986**, *42*, 1633–1640.

(17) Almi, M.; Arduini, A.; Casnati, A.; Pochini, A.; Ungaro, R. Chloromethylation of calixarenes and synthesis of new water soluble macrocyclic hosts. *Tetrahedron* **1989**, *45*, 2177–2182.

(18) Maczynski, A.; Shaw, D. G.; Goral, M.; Wisniewska-Goclowska, B. IUPAC-NIST solubility data series. 82. Alcohols with water—revised and updated: part 1. C4 alcohols with water. *J. Phys. Chem. Ref. Data* **2007**, *36*, 59–132.

(19) Shiraishi, S.; Komiyama, M.; Hirai, H. Immobilization of beta-cyclodextrin on silica-gel. *Bull. Chem. Soc. Jpn.* **1986**, *59*, 507–510.

(20) Fan, M.; Shevchenko, I. V.; Voorhies, R. H.; Eckert, S. F.; Zhang, H.; Lattman, M. Main-group-element calix[4]arenes: variable coordination and conformational isomerism at phosphorus and silicon. *Inorg. Chem.* **2000**, *39*, 4704–4712.

(21) Hajek, F.; Graf, E.; Hosseini, M. W. Multicavitands IV: synthesis of linear koilands obtained by fusion of calix[4]arene derivatives by silicon atoms. *Tetrahedron Lett.* **1996**, *37*, 1409–1412.

(22) Delaigue, X.; Hosseini, M. W.; De Cian, A.; Fischer, J.; Leize, E.; Kieffer, S.; Van Dorsselaer, A. Multicavitands I: synthesis and X-ray crystal structure of a bis p-tert-butylcalix[4]arene fused by two silicon atoms. *Tetrahedron Lett.* **1993**, *34*, 3285–3288.

(23) Shang, S.; Khasnis, D. V.; Burton, J. M.; Santini, C. J.; Fan, M.; Small, A. C.; Lattman, M. From a novel silyl p-tert-butylcalix[4]arene triether to mono-O-alkyl substitution: a unique, efficient, and selective route to mono-O-substituted calix[4]arenes. *Organometallics* **1994**, *13*, 5157–5159.

(24) Stoikov, I.; Mostovaya, O.; Antipin, I.; Konovalov, A.; Grüner, M.; Habicher, W. Synthesis and spatial structure of novel organosilicon derivatives of p-tert-butylthiacalix[4]arene from two-dimensional NMR data. *Russ. Chem. Bull.* **2007**, *56*, 307–312.

(25) Dabrowski, A.; Jaroniec, M. Theoretical foundations of physical adsorption from binary non-electrolytic liquid mixtures on solid surfaces: present and future. *Adv. Colloid Interface Sci.* **1987**, *27*, 211–283.

(26) Jaroniec, M.; Madey, R.; Dabrowski, A. Assessment of microporosity in porous adsorbents by comparing the liquid-solid adsorption isotherms. *Langmuir* **1989**, *5*, 987–990.

(27) Brunauer, S.; Emmett, P. H.; Teller, E. Adsorption of gases in multimolecular layers. *J. Am. Chem. Soc.* **1938**, *60*, 309.

(28) Derylo, A.; Jaroniec, M. Multi-solute adsorption from dilute-solutions on solids. *Chem. Scr.* **1982**, *19*, 108–115.

(29) Choma, J.; Jaroniec, M.; Burakiewicz-Mortka, W.; Gilpin, R. K. Studies of the structural heterogeneity of microporous carbons using liquid/solid adsorption isotherms. *Langmuir* **1993**, *9*, 2555–2561.

(30) Jaroniec, M.; Dabrowski, A.; Toth, J. Multilayer single-solute adsorption from dilute solutions on energetically heterogeneous solids. *Chem. Eng. Sci.* **1984**, *39*, 65–70.

(31) Radke, C. J.; Prausnitz, J. M. Adsorption of organic solutes from dilute aqueous solution on activated carbon. *Ind. Eng. Chem. Fundam.* **1972**, *11*, 445–451.

(32) Terzyk, A. P.; Rychlicki, G.; Cwiertnia, M. S.; Gauden, P. A.; Kowalczyk, P. Effect of the carbon surface layer chemistry on benzene adsorption from the vapor phase and from dilute aqueous solutions. *Langmuir* **2005**, *21*, 12257–12267.

(33) Dohnal, V.; Fenclová, D.; Vrbka, P. Temperature dependences of limiting activity coefficients, Henry's law constants, and derivative infinite dilution properties of lower (C1-C5) 1-alkanols in water. critical compilation, correlation, and recommended data. *J. Phys. Chem. Ref. Data* **2006**, *35*, 1621–1651.

(34) Gupta, A. K.; Teja, A. S.; Chai, X. S.; Zhu, J. Y. Henry's constants of n-alkanols (methanol through n-hexanol) in water at temperatures between 40 and 90 °C. *Fluid Phase Equilib.* **2000**, *170*, 183–192.

(35) Iki, N.; Miyano, S. Can thiacalixarene surpass calixarene? *J. Inclusion Phenom. Macrocyclic Chem.* **2001**, *41*, 99–105.

(36) Kobayashi, K.; Asakawa, Y.; Kikuchi, Y.; Toi, H.; Aoyama, Y. CH-π interaction as an important driving force of host-guest complexation in apolar organic media. Binding of monools and acetylated compounds to resorcinol cyclic tetramer as studied by proton NMR and circular dichroism spectroscopy. *J. Am. Chem. Soc.* **1993**, *115*, 2648–2654.

(37) Sone, T.; Ohba, Y.; Moriya, K.; Kumada, H.; Ito, K. Synthesis and properties of sulfur-bridged analogs of p-tert-butylcalix[4]arene. *Tetrahedron* **1997**, *53*, 10689–10698.

(38) Arena, G.; Contino, A.; Gulino, F. G.; Magri, A.; Sciotto, D.; Ungaro, R. Complexation of small neutral organic molecules by water soluble calix[4]arenes. *Tetrahedron Lett.* **2000**, *41*, 9327–9330.